https://doi.org/10.1016/j.aca.2022.340024

A turn-on hydrazide oxidative decomposition-based fluorescence probe for highly selective detection of Cu^{2+} in tap water as well as cell imaging

Yusuke Okamoto[1], Naoya Kishikawa[2,*], Masayori Hagimori[3], Mahmoud El-Maghrabey[2,4], Shigeru Kawakami[5], Naotaka Kuroda[2]

[1] *School of Pharmaceutical Sciences, Nagasaki University, 1-14 Bunkyo-machi, Nagasaki 852-8521, Japan*

[2] *Department of Analytical Chemistry for Pharmaceutics, Graduate School of Biomedical Sciences, Nagasaki University, 1-14 Bunkyo-machi, Nagasaki, 852-8521, Japan*

[3] *Laboratory of Analytical Chemistry, School of Pharmacy and Pharmaceutical Sciences, Mukogawa Women's University, 11-68 Koshien Kyuban-cho, Nishinomiya 663-8179, Japan*

[4] *Department of Pharmaceutical Analytical Chemistry, Faculty of Pharmacy, Mansoura University, 35116 Mansoura, Egypt*

[5] *Department of Pharmaceutics, Graduate School of Biomedical Sciences, Nagasaki University, 1-7-1 Sakamoto, Nagasaki, 852-8588, Japan*

*** Corresponding author:**

Naoya Kishikawa – *Department of Analytical Chemistry for Pharmaceutics, Graduate School of Biomedical Sciences, Nagasaki University, 1-14 Bunkyo-machi, Nagasaki, 852-8521, Japan;* https://oricd.org/0000-0001-5057-828X; Tel.: +81958192445; fax: +81958192446**;** E-mail address: kishika@nagasaki-u.ac.jp

Abstract

Copper (II) is one of the most important metal ions for the human body that act as a catalytic cofactor for many metalloenzymes and proteins, and its homeostasis disruption could lead to many neurological diseases. The reported probes for Cu (II) determination are mostly based on fluorescence quenching mechanism, which provides low precision and reliability. In the present work, a turn-on fluorescence probe, (*Z*)-1-[2-oxo-2-[2-[1-oxoaceanthrylen-2 (1*H*)-ylidene]hydrazinyl]ethyl]-pyridinium (OAHP), for highly selective detection of Cu^{2+} was developed. Hydrazide moiety of OAHP quenches probe fluorescence; however, upon its reaction with Cu, oxidative cleavage of the hydrazide moiety and intramolecular cyclization occurs, forming oxadiazole derivative with strong fluorescent properties. In this context, OAHP displayed significant fluorescence enhancement with increasing levels of Cu^{2+}. OAHP could detect Cu^{2+} selectively with a detection limit of 18 nM (1.1 ppb). This is the first report for a probe that uses the ability of Cu^{2+} to induce oxidative decomposition of hydrazide with intramolecular cyclization, and it showed exceptional selective performance and exquisite sensitivity. Next, the method was applied successfully for monitoring Cu2+ in tap water samples with good accuracy (found% of 95.8 - 101.5 %) and precisions (RSD<10%). Finally, OAHP was successfully applied for imaging Cu^{2+} in living cells, and this result indicates the potential of OAHP for selective detection of Cu^{2+} in complicated matrices.

Keywords: Cu^{2+} detection, Cell imaging, Hydrazide derivatives, Aceanthrenequinone**,** Turn on fluorescence probe

1. Introduction

Copper is considered the third most essential trace element in the human body after iron and zinc. Copper (Ⅱ) ion (Cu^{2+}) is closely associated with various fundamental physiological processes, and its homeostasis is vitally important to living organisms [1–3]. It also plays a crucial role as catalytic cofactors for many metalloenzymes and proteins, including tyrosinase and amine oxidase [4]. It has been reported that the depletion of Cu^{2+} leads to several serious diseases, such as Parkinson's disease [5] and Alzheimer's disease [6,7]. Conversely, excessive levels of Cu^{2+} exhibit oxidative stress leading to toxicity to human health. Also, the homeostasis imbalance of Cu^{2+} is related to the pathogenesis of neurodegenerative diseases, including prion, Menkes, Wilson diseases, and familial amyotrophic lateral sclerosis [8–10]. From these backgrounds, developing a simple, sensitive, and selective analytical method for Cu^{2+} should be important.

Among analytical methods for metal ions, the fluorescence probe-based method is advantageous in the aspect of simplicity, cost-effectiveness, and applicability for imaging compared with instrumental methods such as atomic emission spectrometry [11], atomic absorption spectrometry [12], and inductively coupled plasma-mass spectrometry [13]. Hence, till now, various fluorescence probes for detecting Cu^{2+} have been developed. However, previously reported probes have many limitations, for example, complicated synthetic methods [14,15], large molecular size [16], low water solubility [17], and undesirable

responsiveness to interfering metal ions [18–20]. Also, most of the probes exhibit a fluorescence turn-off response towards Cu^{2+} [21–24]. These turn-off type probes restrict their application in fluorescence imaging. Additionally, several probes have been developed based on the formation of a chelate complex with Cu^{2+}. However, such chelating probes are susceptible to disturbance by other metal ions because ligand moiety cannot interact selectively with Cu^{2+} [25,26]. Thus, the development of easily synthesizable, selective, and dual reaction-based turn-on fluorescence probes for Cu^{2+} is still interest.

In the present study, we developed a turn-on fluorescent probe for Cu^{2+}, (*Z*)-1-[2-oxo-2-[2-[1-oxoaceanthrylen-2(1*H*)-ylidene]hydrazinyl]ethyl]-pyridinium (OAHP). OAHP could be synthesized easily in a one-step process (Scheme 1). OAHP itself possesses very weak fluorescence due to the isomerization of the hydrazide moiety. Upon its reaction with Cu^{2+} substantial enhancement in fluorescence occurs. Thus, OAHP can measure Cu^{2+} levels based on fluorescence enhancement. This could be attributed to Cu^{2+} induced oxidative cleavage of the hydrazide moiety, and intramolecular cyclization occurs, forming oxadiazole derivative with strong fluorescent properties. Similarly, Cu^{2+} was used recently in the field of organic synthesis as a catalyst for the oxidative decomposition of the hydrazide moiety, followed by intramolecular amination with hydrazones [27]. In our case, a similar mechanism occurs, where the resulted hydrazone moiety was further oxidized by Cu^{2+} into a diazo group followed by intramolecular cyclization with the adjacent carbonyl group forming oxadiazole.

Thus, the sensing for copper occurs through a two-step reaction, hydrolysis, and oxidation, which were followed by consequence intramolecular cyclization, making the probe very selective to Cu^{2+}. In this study, the quantitativeness and selectivity of OAHP for Cu^{2+} were evaluated. Besides, further application of OAHP in fluorescence imaging was studied in Hep G2 cells through a fluorescence microscope, proposing a potential fluorescence probe for Cu^{2+} *in vivo*.

2. Experimental

2.1. Materials and instrumentation

Aceanthrenequinone (ACAQ) was purchased from Sigma-Aldrich (ST. Louis, USA). Girard's Reagent P (1-(hydrazino-carbonyl methyl)pyridinium chloride) was purchased from Tokyo Chemical Industries (Tokyo, Japan). Copper(Ⅱ) acetate monohydrate was derived from Kishida Chemical Co., Ltd (Osaka, Japan). All other metal reagents (Na_2SO_4, K_2SO_4, $BaCl_2 \cdot 2H_2O$, $MgSO_4 \cdot 7H_2O$, $CaCl_2$, $SrCl_2 \cdot 6H_2O$, $CrK(SO_4)_2 \cdot 12H_2O$, $CoCl \cdot 6H_2O$, $MnCl_2 \cdot 4H_2O$, $FeSO_4 \cdot 7H_2O$, $Fe(NO_3)_3 \cdot 9H_2O$, $NiCl_2 \cdot 6H_2O$, CuI, $Zn(CH_3COO)_2 \cdot 2H_2O$, $AlK(SO_4) \cdot 12H_2O$) were of analytical grade. Water was distilled and purified by Pureline WL-100 and Auto Still WG203 (Yamato, Tokyo). Fluorescence measurements were carried out on RF-1500 (Shimadzu, Kyoto, Japan). Fluorescence imaging was performed on BZ-X710 All-in-One Fluorescence Microscope (KEYENCE).

2.2. Synthesis of OAHP

Aceanthrenequinone (46 mg, 0.2 mmol) and Girard's Reagent P (37 mg, 0.2 mmol) were dissolved in a solvent mixture of 2 mL 1,4-dioxane and 2 mL acetic acid. After the reaction at 90 ℃ for 7 h, precipitated crystals were filtered. Filtered crystals were washed with 8 mL of 1,4-dioxane to give the pure product as a yellowish solid; yield 78.1%, Elemental analysis: calculated for $C_{23}H_{16}N_3O_2Cl \cdot 0.75CH_3COOH$, calculated: C, 65.85%; H, 4.29%; N, 9.40%; found: C, 65.85%; H, 4.28%; N, 9.69%; FAB-MS (*m/z*) found: 366, calculated: 366 $[M]^+$; ESI-MS (*m/z*) found: 366.1, calculated: 366 (Figure S1); ^{1}H NMR (500 MHz, CD_3OD) 6.307 (s, 2H, O=C-CH_2), 7.697-7.751 (m, 2H, Ar-H), 7.806-7.838 (t, 1H, Ar-H), 7.939-7.952 (d, 1H, Ar-H), 8.163-8.180 (d, 1H, Ar-H), 8.225-8.273 (m, 3H, Ar-H), 8.733-8.764 (t, 1H, Ar-H), 8.902 (s, 1H, Ar-H), 8.925-8.942 (d, 1H, Ar-H), 9.056-9.067 (d, 2H, Ar-H) (Figure S2 a,b).

2.3. General procedure for the fluorescence studies

OAHP stock solution (2.0 mM) was dissolved in methanol and then diluted to 50 μM in methanol. All metal ions (Cu^{2+}, Na^+, K^+, Ba^{2+}, Mg^{2+}, Ca^{2+}, Sr^{2+}, Cr^{3+}, Co^{2+}, Mn^{2+}, Fe^{2+}, Fe^{3+}, Ni^{2+}, Cu^+, Zn^{2+}, Al^{3+}) were prepared as aqueous solution, and then were diluted with methanol at 50 μM for the fluorescence experiments. An aliquot of 200 μL OAHP was mixed with 200 μL metal ion and left at room temperature for 60 min. Then, it was diluted with 1.6 mL methanol. The fluorescence measurement was carried out with excitation at 370 nm.

2.4. Analysis of Cu^{2+} in tap water.

Tap water samples were filtered and then spiked with different concentrations of Cu^{2+}. Then, 200 μL of spiked tap water was mixed with 200 μL of 50 μM OAHP, and the reaction mixture was allowed to react at room temperature for 30 min. Afterward, it was diluted with 1.6 mL methanol. The fluorescence measurement was carried out with excitation at 370 nm.

2.5. Cytotoxicity assay

HepG2 cells (sourced from Riken Cell Bank, Tsukuba, Japan) were seeded 5×10^3 /cells in a 96-well culture plate. After being cultured for 24 hours, the cells were treated with 10 μM, 20 μM, 50 μM, 100 μM, and 200 μM OAHP, dissolved in 5 % aqueous methanol at 37 ℃ for 2 or 4 hours. 5-[2,4-Bis(sodiooxysulfonyl)phenyl]-3-(2-methoxy-4-nitrophenyl)-2-(4-nitrophenyl)-2*H*-tetrazolium (WST-8) was added to each well, and the cells were cultured for 1 hour. Then, absorbances at 450 nm were recorded by a microplate reader.

2.6. Cell culture and imaging

HepG2 cells were cultured in Dulbecco's Modified Eagle's Medium (DMEM) supplemented with 10% fetal bovine serum (FBS) and 1% antibiotics (penicillin and streptomycin) at 37 ℃ under a humidified atmosphere of 5% CO_2 and 95% air. Subconfluent cells were replaced in a fresh medium using trypsin. A subculture was performed every four days. Approximately 5.0×10^4 cells were seeded. After 24 hours, the cells were treated with 100 μM $CuSO_4$ at the above condition for 30 min and washed with PBS to remove

extracellular $CuSO_4$. OAHP (100 μM) dissolved in 5% methanol aqueous solution was incubated with the cells for 2 hours and then washed with PBS to remove excess OAHP. Cells treated only with OAHP were selected as control. Fluorescence imaging was performed with BZ-X710 All-in-One Fluorescence Microscope (KEYENCE).

3. Results and discussion

3.1. Fluorescence spectral changes and sensing of OAHP after addition of Cu^{2+}

Firstly, the fluorescence spectral characteristics of OAHP were investigated in the absence and presence of Cu^{2+}. As shown in Figure 1, OAHP exhibited extremely weak fluorescence because of the non-radiative deactivation through rapid isomerization of the O=C-N bond in the excited state. Meanwhile, visible fluorescence with a maximum emission at 490 nm was observed after the addition of Cu^{2+} upon excitation at 370 nm.

When EDTA was added to the solution after the reaction, the fluorescence intensity was not changed (Figure 2), which proves that the mechanism for Cu^{2+} sensing is not complex formation and indicates that a chemical reaction has occurred. Cu^{2+} was previously used in the organic synthesis of 1*H*-Indazoles and 1*H*-Pyrazoles through catalysis of the oxidative decomposition of the amide bond of hydrazides followed by intramolecular cyclization [27]. Then, it was found that Cu^{2+} reacts similarly with OAHP producing aceantherene oxadiazole derivative. To elucidate the reaction mechanism and the structure of the fluorescent product,

OAHP before and after its reaction with Cu^{2+} was analyzed by ESI-MS (JMS-DX 303 electron impact mass spectrometer, JEOL, Tokyo, Japan). OAHP alone exhibited a molecular ion peak at 366.1, and upon its reaction with Cu^{2+}, the peak at 366.1 was greatly decreased and a molecular ion peak was observed at m/z = 244.2 that corresponds to $[M]^+$ of aceanthrene-oxadiazole derivative (Figure 3). Then, the mechanism was proposed to occur as illustrated in Scheme 2B. At first, Cu^{2+} will hydrolyze the amide group of the hydrazide moiety forming aceanthraquinone monohydrazone. Then, the formed hydrazone moiety is liable to oxidation [28], thus, it will be oxidized by Cu^{2+} [29] forming a diazo compound. As the formed diazo compound has an α-carbonyl group adjacent to the diazo group, it undergoes intramolecular cyclization forming an oxadiazole derivative [30].

To prove that the mechanism of sensing includes an oxidation process, we tested the effect of an antioxidant, ascorbic acid, and we found that it inhibits the reaction to about 50% if added initially. However, when ascorbic acid was added after the reaction completion, no change occurred in the fluorescence intensity (Figure 2). Additionally, when we tested the reaction of the reduced form of copper (cuprous iodide), no fluorescence was observed (Figure 2), which demonstrates that copper should be in its oxidation state to react. Additionally, we measured the fluorescence of the substrate aceanthrenequinone either alone or in the presence of hydrazine. In both cases, we found that no fluorescence is produced, which demonstrates that aceanthrenequinone and its monohydrazone derivative are not

responsible for the fluorogenic response (Figure 2). In addition to the previous mass and fluorescence data, the occurrence of intramolecular cyclization is a must for the formation of a fluorescent compound to inhibit the isomerization of the C=N bond of the hydrazone moiety [31]. Hence the fluorescence product was deduced as shown in Scheme 2.

3.2. Optimization and validation of the proposed OAHP probe for sensing Cu^{2+} and application to Cu^{2+} control in tap water

At first, we studied the reaction between OAHP and Cu^{2+} in methanol. The reaction proceeds well in methanol and reaches nearly 87 % completion within 30 min (Figure 4a). Then, we studied the reaction in an aqueous methanol mixture, and good fluorescence intensity was obtained in the aqueous methanol mixture till 50% aqueous methanol. These results demonstrate that our probe could be used in aqueous conditions with water content up to 50% (Figure 4b).

The calibration experiment was performed by the addition of different concentrations of Cu^{2+} to OAHP. As shown in Figure 5, the fluorescence intensity at 490 nm increased gradually with increasing the concentration of Cu^{2+}. A sufficient linear relationship (r^2 = 0.992) between the concentration of Cu^{2+} and the fluorescence intensity was obtained in the range of 0.05–2.0 μM. The linear regression equation was FI = 641.4 C + 38.1, where FI and C represent the fluorescence intensity and the concentration of Cu^{2+}, respectively. The

detection limit, defined as 3σ/K, was calculated and found to be 0.018 μM (1.1 ppb), where σ is the blank standard deviation and K is the slope of the regression equation [32]. Next, to confirm the reliability of the calculated LOD, we have tried to detect 18 nM (1.1 ppb) practically, and it yielded fluorescence intensity 1.5 of that of blank, which is a noticeable change in blank more than three times its standard deviation (3σ). Hence, 1.1 ppm could be considered the actual practical LOD. This LOD is lower than most of the previously reported probes for Cu^{2+} in recent years (Table. 1), which demonstrates the excellent sensitivity of the developed probe. Moreover, the upper limit of Cu^{2+} in drinking water is 1.3 ppm [33], which is 1000 times higher than our detection limit, demonstrating the suitability of our method for monitoring Cu^{2+} level in tap water, especially our sensing reaction could proceed well in the presence of water. Consequently, the accuracy and precision of the measurement of Cu^{2+} at different spiked concentrations in tap water were studied, and good accuracy (found% of 95.8 - 101.5 %) and sufficient intra- and inter-day precisions (<10%) were confirmed as listed in Table 2.

3.3.Selectivity of OAHP to Cu^{2+} vs. other metal ions

To investigate the reaction selectivity of OAHP with Cu^{2+}, the fluorescence changes upon addition of Cu^{2+}, Na^{+}, K^{+}, Ba^{2+}, Mg^{2+}, Ca^{2+}, Sr^{2+}, Cr^{3+}, Co^{2+}, Mn^{2+}, Fe^{2+}, Fe^{3+}, Ni^{2+}, Cu^{+}, Zn^{2+} and Al^{3+} were examined. As shown in Figure 6, OAHP indicated significant fluorescence enhancement towards only Cu^{2+}. Even Cu^{+} did not produce any significant

fluorescence upon its interaction with the probe. This excellent selectivity could also be observed from the photograph of OAHP after the addition of Cu^{2+} (Figure 6b). In addition, a competitive experiment was carried out in the presence of the metal ions mentioned above. It was found that these metal ions have a negligible effect on the fluorescence enhancement of OAHP by Cu^{2+} (Figure 7). These results indicated that OAHP has excellent selectivity towards Cu^{2+}.

3.4. Fluorescence imaging of Cu^{2+}

We evaluated the practicability of OAHP for fluorescence imaging of intracellular Cu^{2+} in HepG2 cells. At first, the cytotoxicity of OAHP against living cells was tested by WST-8 assay. Although HepG2 cells were treated with 10-200 μM of OAHP for 2 and 4 hours, no obvious cytotoxicity with cell viability over 95% was observed until 100 μM and decreased to 87 % at 200 μM OAHP, which is still acceptable viability (Figure 8 and Figure S3). Then, we decided to use 100 μM OAHP for fluorescence imaging. Figure 9 reveals the photographs of HepG2 cells obtained with fluorescence microscopy. HepG2 cells incubated with 100 μM OAHP alone for 2 hours showed very weak fluorescence. While cells incubated with 100 μM Cu^{2+} for 30 min, before the addition of 100 μM OAHP, showed a significant increase in the fluorescence from the intracellular domain. The green fluorescence intensities in the control cells and cells preincubated with Cu^{2+} were measured using Image J software, and the results are shown in Figure S3. It was found that the produced green fluorescence intensity was

increased about six times in Cu^{2+} treated cells than in the control ones. Then, we tried to image 20, 50, and 100 μM $CuSO_4$ in cells, and the results are shown in Figure S4. We have found an excellent linear relationship between $CuSO_4$ concentration and integrated green fluorescence intensity (Figure S4C). Blank experiments were carried out simultaneously using OAHP only (n=3). Afterward, the integrated green fluorescence intensities for blank experiments were measured, and the standard deviation was calculated. The LOD of Cu^{2+} imaging in cells was calculated by using the formula 3σ/K, where σ is the blank standard deviation and K is the slope of the regression equation. The LOD was found to be 0.35 μM (22 ppb). These results suggest that OAHP can be used to efficiently image intracellular Cu^{2+} levels in living cells with good sensitivity. $CuSO_4$ LD 50 for cells is about 1380 μM, and our LOD is about 4000 times lower than this level which proves the excellent performance and great applicability of our method for Cu^{2+} imaging [34].

3.5.Comparison of the performance of OAHP vs. previously reported ones for Cu^{2+} sensing

We compared the performance of OAHP with previously reported probes [19,22–26,35–37] as summarized in Table 1. Most of the previously reported probes for Cu^{2+} require laborious multistep synthesis and purification process in contrast to our probe, which was synthesized in one step and easily purified through filtration. Regarding the performance, our probe showed excellent sensitivity with an LOD of 18 nM (1.1 ppb), which is 8-550

times more sensitive than most of the previously reported probes for Cu^{2+} [19,22–26,35,36]. Only the naphthalimide probe showed similar sensitivity to our designed probe; however, the naphthalimide probe has very poor selectivity, and various cations can interfere with the measurement of Cu^{2+} [37]. Also, this probe has a very short stokes shift of about 24 nm. Additionally, most of the previously reported probes for Cu^{2+} are based on fluorescence turn-off mechanisms [19,22–24,35,36] that provide low precision and reliability and limit their applicability. Moreover, fluorescence turn-off probes are not suitable for imaging applications. Regarding the measurement wavelength, our probe has long excitation and emission wavelengths which are longer or comparable to previously reported ones with a good stokes shift of 120 nm. At the same time, our probe has a unique advantage which is its exceptional selectivity to Cu^{2+} in the presence of many competing cations.

At last, the cost-effectiveness of the probe was evaluated through the calculation of its possible price. From the synthesis and purification procedures of OAHP, the cost-determining factors are the used substrates, namely aceanthrenequinone and Girard reagent P, as the used solvents are cheap and the used purification procedure is very simple. One gram of aceanthrenequinone (4.3 mmol) costs 78 USD (Sigma Aldrich price, https://www.krackeler.com/catalog/sigma/ALDRICH/327972), while 25 g of Girard reagent P (133 mmol) cost 122 USD (TCI price, https://www.tcichemicals.com/US/en/p/G0030), hence 4.3 mmol cost about 4 USD. Thus, using 4.3 mmol of the substrates will cost 82 USD, and

with the obtained yield (78 %), the obtained amount of OAHP will be about 3.4 mmol (about 1.24 g). Hence, we can assume that 1 g of OAHP will cost about 70 USD, which is similar to or even cheaper than the cost of its used substrate, aceanthrenequinone, proving the cost-effectiveness of the developed probe.

4. Conclusion

In the present study, a new highly selective turn-on fluorescence probe for detecting Cu^{2+}, OAHP, was developed. Although the fluorescence of OAHP is quenched by the isomerization of hydrazide, the fluorescence recovery can be achieved after its reaction with Cu^{2+} through the oxidative cleavage of the hydrazide moiety and intramolecular cyclization that eventually forms oxadiazole derivative with strong fluorescent properties. OAHP could detect Cu^{2+} sensitively with a detection limit of 1.1 ppb. OAHP exhibited excellent selectivity to Cu^{2+} in the presence of coexisting other metal ions. Next, the method was applied successfully for the determination of Cu^{2+} in tap water. At last, OAHP was successfully applied to visualize intracellular Cu^{2+} in living HepG2 cells.

Acknowledgment

In this work, we used the research equipment shared in the MEXT Project to promote public utilization of advanced research infrastructure (Program for supporting the introduction of the new sharing system) Grant Number JPMXS0422500320.

Reference

[1] E.L. Que, D.W. Domaille, C.J. Chang, Metals in neurobiology: Probing their chemistry and biology with molecular imaging, Chem. Rev. 108 (2008) 1517–1549.

[2] E. Gaggelli, H. Kozlowski, D. Valensin, G. Valensin, Copper homeostasis and neurodegenerative disorders (Alzheimer's, Prion, and Parkinson's Diseases and Amyotrophic Lateral Sclerosis), Chem. Rev. 106 (2006) 1995–2044.

[3] A.K. Boal, A.C. Rosenzweig, Structural biology of copper trafficking, Chem. Rev. 109 (2009) 4760–4779.

[4] T.G. Gaule, M.A. Smith, K.M. Tych, P. Pirrat, C.H. Trinh, A.R. Pearson, P.F. Knowles, M.J. McPherson, Oxygen activation switch in the copper amine oxidase of Escherichia coli, Biochemistry. 57 (2018) 5301–5314.

[5] J.C. Lee, H.B. Gray, J.R. Winkler, Copper(II) binding to α-synuclein, the Parkinson's protein, J. Am. Chem. Soc. 130 (2008) 6898–6899.

[6] K.J. Barnham, C.L. Masters, A.I. Bush, Neurodegenerative diseases and oxidative stress, Nat. Rev. Drug Discov. 3 (2004) 205–214.

[7] C. Cheignon, P. Faller, D. Testemale, C. Hureau, F. Collin, Metal-catalyzed oxidation of Aβ and the resulting reorganization of Cu binding sites promote ROS production, Metallomics. 8 (2016) 1081–1089.

[8] R.R. Crichton, D.T. Dexter, R.J. Ward, Metal based neurodegenerative diseases—From molecular mechanisms to therapeutic strategies, Coord. Chem. Rev. 252 (2008) 1189–1199.

[9] D.J. Waggoner, T.B. Bartnikas, J.D. Gitlin, The role of copper in neurodegenerative disease, Neurobiol. Dis. 6 (1999) 221–230.

[10] Y.-F. Tan, N. O'Toole, N.L. Taylor, A.H. Millar, Divalent metal ions in plant mitochondria and their role in interactions with proteins and oxidative stress-induced

damage to respiratory function, Plant Physiol. 152 (2010) 747–761.

[11] S.L.. Ferreira, A.S. Queiroz, M.S. Fernandes, H.C. dos Santos, Application of factorial designs and Doehlert matrix in optimization of experimental variables associated with the preconcentration and determination of vanadium and copper in seawater by inductively coupled plasma optical emission spectrometry, Spectrochim. Acta Part B At. Spectrosc. 57 (2002) 1939–1950.

[12] Y. Yamini, N. Alizadeh, M. Shamsipur, Solid phase extraction and determination of ultra trace amounts of mercury(II) using octadecyl silica membrane disks modified by hexathia-18-crown-6-tetraone and cold vapour atomic absorption spectrometry, Anal. Chim. Acta. 355 (1997) 69–74.

[13] C.F. Harrington, S.A. Merson, T.M. D' Silva, Method to reduce the memory effect of mercury in the analysis of fish tissue using inductively coupled plasma mass spectrometry, Anal. Chim. Acta. 505 (2004) 247–254.

[14] J. Huang, M. Liu, X. Ma, Q. Dong, B. Ye, W. Wang, W. Zeng, A highly selective turn-off fluorescent probe for Cu(<scp>ii</scp>) based on a dansyl derivative and its application in living cell imaging, RSC Adv. 4 (2014) 22964–22970.

[15] Y.-G. Gao, Q. Tang, Y.-D. Shi, Y. Zhang, Z.-L. Lu, 1,8-Naphthalimide modified [12]aneN3 compounds as selective and sensitive probes for Cu^{2+} ions and ATP in aqueous solution and living cells, Talanta. 152 (2016) 438–446.

[16] Y. Zhou, J. Zhang, H. Zhou, Q. Zhang, T. Ma, J. Niu, A new rhodamine B-based "off–on" fluorescent chemosensor for Cu^{2+} in aqueous media, J. Lumin. 132 (2012) 1837–1841.

[17] Z. Kowser, C.-C. Jin, X. Jiang, S. Rahman, P.E. Georghiou, X.-L. Ni, X. Zeng, C. Redshaw, T. Yamato, Fluorescent turn-on sensors based on pyrene-containing Schiff base derivatives for Cu^{2+} recognition: spectroscopic and DFT computational studies,

Tetrahedron. 72 (2016) 4575–4581.

[18] M.M. Yu, Z.X. Li, L.H. Wei, D.H. Wei, M.S. Tang, A 1,8-Naphthyridine-based fluorescent chemodosimeter for the rapid detection of Zn 2+ and Cu 2+, Org. Lett. 10 (2008) 5115–5118.

[19] B. Zhang, H. Liu, F. Wu, G. Hao, Y. Chen, C. Tan, Y. Tan, Y. Jiang, A dual-response quinoline-based fluorescent sensor for the detection of Copper (II) and Iron(III) ions in aqueous medium, Sensors Actuators B Chem. 243 (2017) 765–774.

[20] Y. Wang, H. Wu, W.N. Wu, S.J. Li, Z.H. Xu, Z.Q. Xu, Y.C. Fan, X.L. Zhao, B.Z. Liu, An AIRE active Schiff base bearing coumarin and pyrrole unit: Cu^{2+} detection in either solution or aggregation states, Sensors Actuators B Chem. 260 (2018) 106–115.

[21] S. Joshi, S. Kumari, A. Sarmah, R. Sakhuja, D.D. Pant, Solvatochromic shift and estimation of dipole moment of synthesized coumarin derivative: Application as sensor for fluorogenic recognition of Fe^{3+} and Cu^{2+} ions in aqueous solution, J. Mol. Liq. 222 (2016) 253–262.

[22] Y. Peng, Y.-M. Dong, M. Dong, Y.-W. Wang, A selective, sensitive, colorimetric, and fluorescence probe for relay recognition of fluoride and Cu(II) ions with “off–on–off” switching in ethanol–water solution, J. Org. Chem. 77 (2012) 9072–9080.

[23] H. Liu, B. Zhang, C. Tan, F. Liu, J. Cao, Y. Tan, Y. Jiang, Simultaneous bioimaging recognition of Al^{3+} and Cu^{2+} in living-cell, and further detection of F− and S2− by a simple fluorogenic benzimidazole-based chemosensor, Talanta. 161 (2016) 309–319.

[24] P. Torawane, S.K. Sahoo, A. Borse, A. Kuwar, A new Schiff base as a turn-off fluorescent sensor for Cu^{2+} and its photophysical properties, Luminescence. 32 (2017) 1426–1430.

[25] F. Ge, H. Ye, J.Z. Luo, S. Wang, Y.J. Sun, B.-X. Zhao, J.Y. Miao, A new fluorescent and colorimetric chemosensor for Cu(II) based on rhodamine hydrazone and ferrocene

unit, Sensors Actuators B Chem. 181 (2013) 215–220.

[26] J.-Z. Ge, Y. Zou, Y.-H. Yan, S. Lin, X.-F. Zhao, Q.-Y. Cao, A new ferrocene–anthracene dyad for dual-signaling sensing of Cu(II) and Hg(II), J. Photochem. Photobiol. A Chem. 315 (2016) 67–75.

[27] G. Zhang, Q. Fan, Y. Zhao, C. Ding, Copper-Promoted Oxidative Intramolecular C-H Amination of Hydrazones to Synthesize 1 H -Indazoles and 1 H -Pyrazoles Using a Cleavable Directing Group, European J. Org. Chem. 2019 (2019) 5801–5806.

[28] S.M. Nicolle, C.J. Moody, Potassium N-iodo p-toluenesulfonamide (TsNIK, Iodamine-T): A new reagent for the oxidation of hydrazones to diazo compounds, Chem. - A Eur. J. 20 (2014) 4420–4425.

[29] K. Sreenath, Z. Yuan, M. Macias-Contreras, V. Ramachandran, R.J. Clark, L. Zhu, Dual role of acetate in copper(II) acetate catalyzed dehydrogenation of chelating aromatic secondary amines: A kinetic case study of copper-catalyzed oxidation reactions, Eur. J. Inorg. Chem. 2016 (2016) 3728–3743.

[30] T.L. Gilchrist, Product Class 5: 1,2,3-Oxadiazoles, in: Storr, Gilchrist (Eds.), Categ. 2, Hetarenes Relat. Ring Syst., Georg Thieme Verlag, Stuttgart, 2004: pp. 109–125.

[31] J.S. Wu, W.M. Liu, X.Q. Zhuang, F. Wang, P.F. Wang, S.-L. Tao, X.H. Zhang, S.K. Wu, S.T. Lee, Fluorescence turn on of coumarin derivatives by metal cations: A new signaling mechanism based on C=N isomerization, Org. Lett. 9 (2007) 33–36.

[32] M. El-Maghrabey, N. Kishikawa, S. Harada, K. Ohyama, N. Kuroda, Quinone-based antibody labeling reagent for enzyme-free chemiluminescent immunoassays. Application to avidin and biotinylated anti-rabbit IgG labeling, Biosens. Bioelectron. 160 (2020) 112215.

[33] R. Manne, M.M.R.M. Kumaradoss, R.S.R. Iska, A. Devarajan, N. Mekala, Water quality and risk assessment of copper content in drinking water stored in copper

container, Appl. Water Sci. 12 (2022) 27.

[34] P.B. Tchounwou, C. Newsome, J. Williams, K. Glass, Copper-Induced Cytotoxicity and Transcriptional Activation of Stress Genes in Human Liver Carcinoma (HepG(2)) Cells, Met. Ions Biol. Med. 10 (2008) 285–290.

[35] N. Roy, A. Dutta, P. Mondal, P.C. Paul, T. Sanjoy Singh, Coumarin based fluorescent probe for colorimetric detection of Fe^{3+} and fluorescence turn on-off response of Zn^{2+} and Cu^{2+}, J. Fluoresc. 27 (2017) 1307–1321.

[36] X. Wu, Z. Guo, Y. Wu, S. Zhu, T.D. James, W. Zhu, Near-infrared colorimetric and fluorescent Cu 2+ sensors based on indoline–benzothiadiazole derivatives via formation of radical cations, ACS Appl. Mater. Interfaces. 5 (2013) 12215–12220.

[37] Z. Xu, Y. Xiao, X. Qian, J. Cui, D. Cui, Ratiometric and selective fluorescent sensor for Cu II based on internal charge transfer (ICT), Org. Lett. 7 (2005) 889–892.

Table 1 Comparison of interfering metal ion, wavelength, and LOD obtained from various fluorescent sensors for the detection of Cu^{2+}.

Structure	**Type**	**Interfering metals**	**Wavelength (λex/λem, nm)**	**Detection limit (μM)**	**Ref**
Quinoline	Turn-off	Fe^{3+}	370/508	0.14	[19]
Iminocoumarin-benzothiazole	Turn-off	Co^{2+}, Mn^{2+}, Ag^{+}	460/523	2.5	[22]
Benzoimidazole	Turn-off	Al^{3+}	355/425	0.54	[23]
Phenylenebis-azanylylidene	Turn-off	Al^{3+}, Fe^{2+}, Fe^{3+}, Hg^{2+}	386/554	0.35	[24]
Rhodamine hydrazine	Turn-on	Hg^{2+}	550/595	0.72	[25]
Ferrocene–anthracene dyad	Turn-on	Hg^{2+}	360/419	1.9	[26]
Coumarin	Turn-off	Zn^{2+}	355/428	10	[35]
Indoline-benzothiadiazole	Turn-off	Fe^{3+}	529/750	1.03	[36]
Naphthalimide	ICT Turn-on	Co^{2+}, Fe^{2+}, Ni^{2+}, Ag^{+}	451/475	0.01	[37]
OAHB	Turn-on	Nothing	370/490	0.018	This work

Table 2. Accuracy and precision data of the proposed method.

Cu^{2+} (μM)	Intra-day (n=5)		Inter-day (n=5)	
	Accuracy (Found%)	**Precision (RSD%)**	**Accuracy (Found%)**	**Precision (RSD%)**
0.5	97.8	5.8	95.8	9.5
1.0	101.5	4.9	101.4	8.4
2.0	99.8	3.8	99.8	4.1

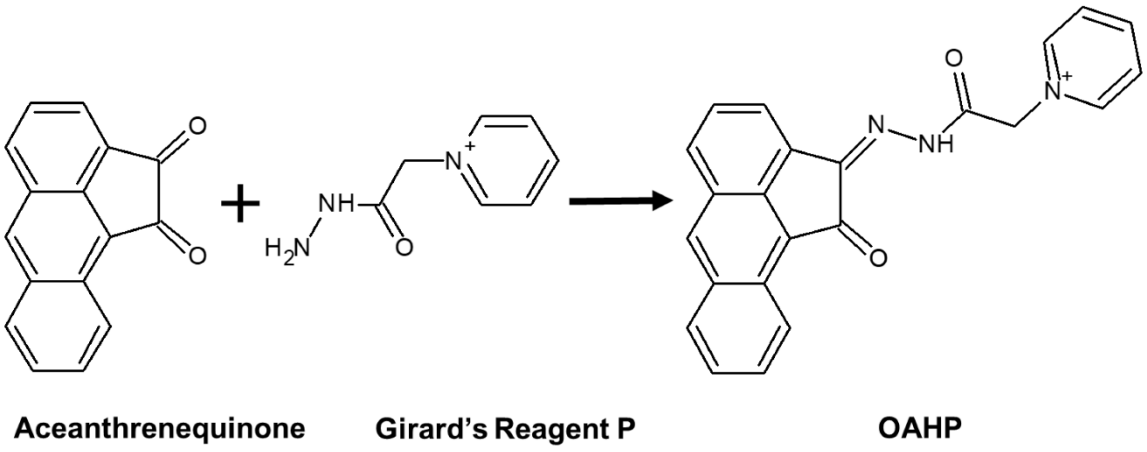

Scheme 1. Synthesis of OAHP.

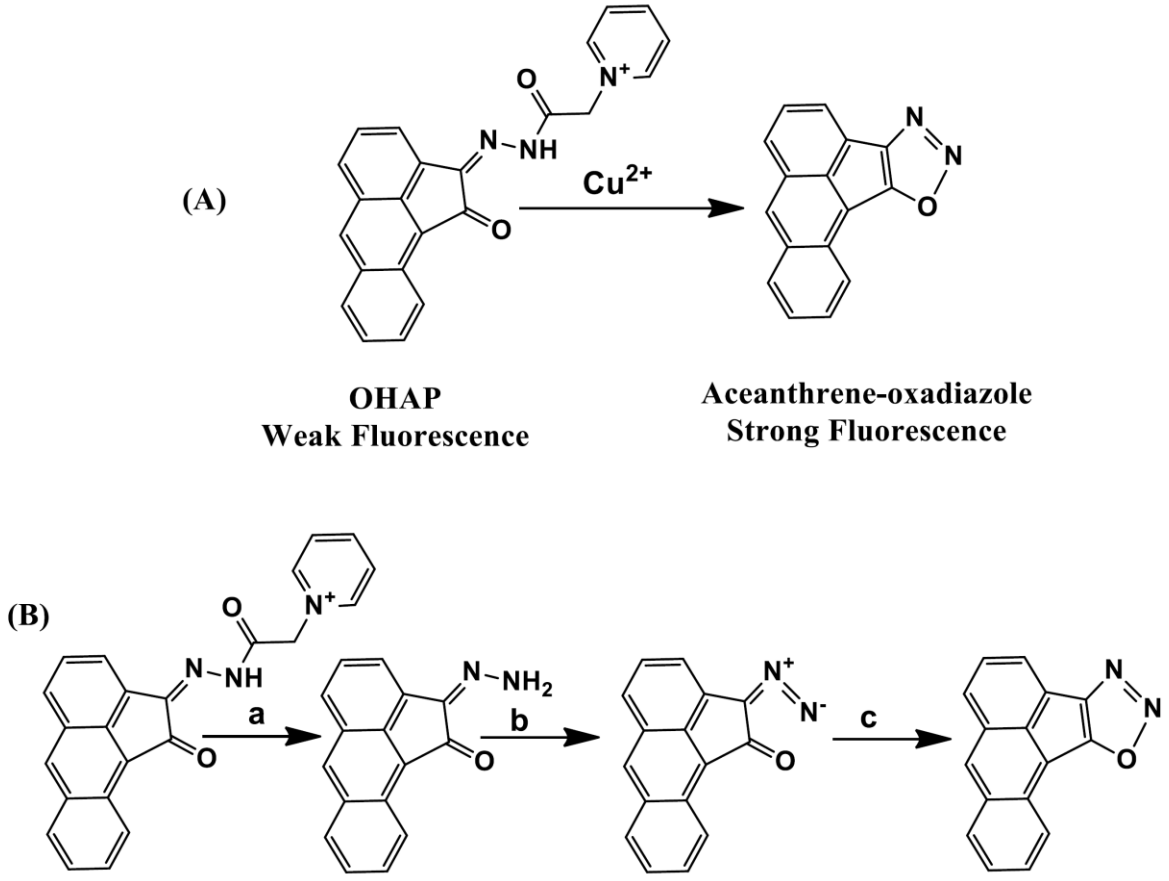

Scheme 2. The proposed reaction of OAHP with Cu^{2+}, where (A) shows the fluorogenic reaction scheme and (B) shows the detailed mechanism of the reaction, which includes (a) hydrolysis of the amide group of the hydrazide moiety, b(b)oxidation of the hydrazone group into a diazo group, and (c) cyclization of the diazo group with the α-carbonyl group forming oxadiazole compound.

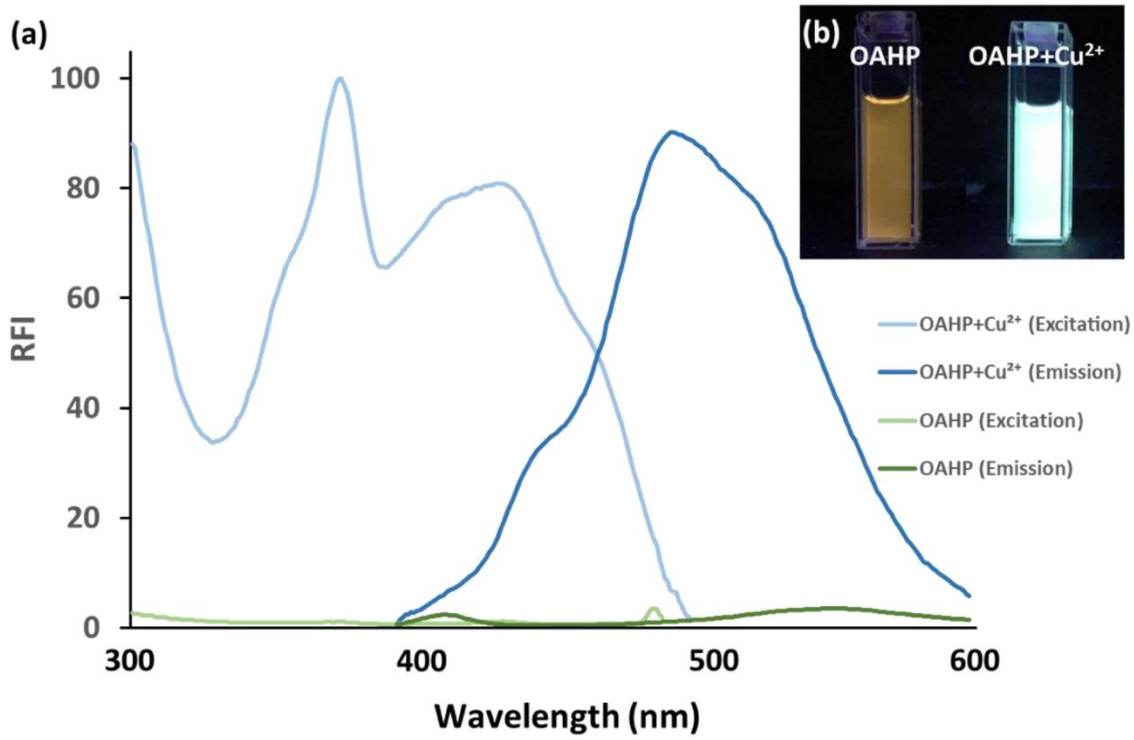

Figure 1. (a) Fluorescence spectra change of OAHP (5 μM, final concentration) and addition of Cu^{2+} (2 μM final concentration), (b) Photograph of OAHP (5.0 μM) and upon addition of Cu^{2+} (2.0 μM).

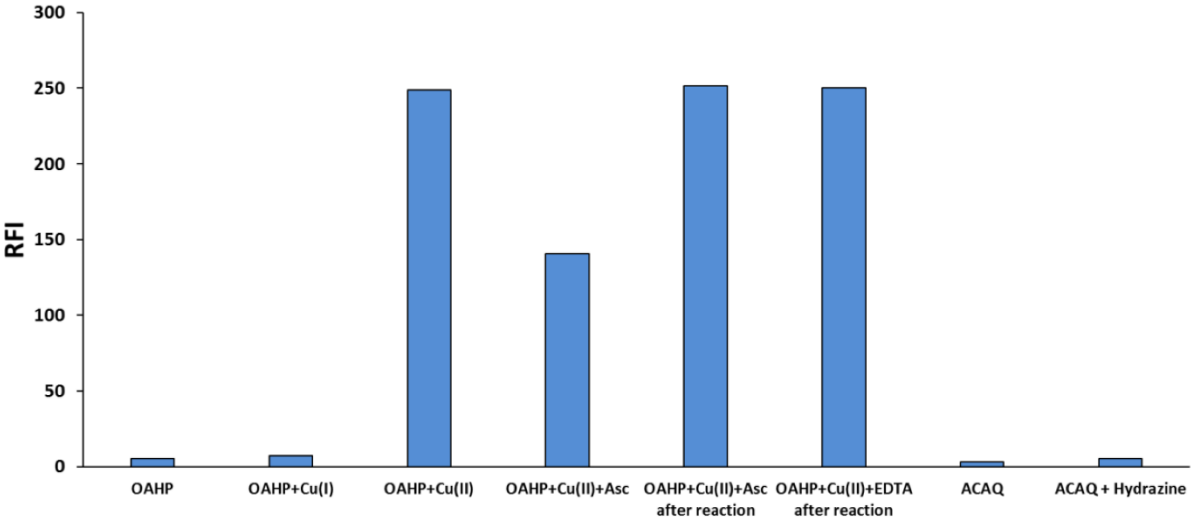

Figure 2. Investigation of the fluorogenic reaction between OAHP and Cu(II) through measuring the fluorescence of OAHP alone and after its mixing with Cu(I), Cu(II) alone, or after the addition of ascorbic acid or EDTA, ACAQ either alone or after adding hydrazine

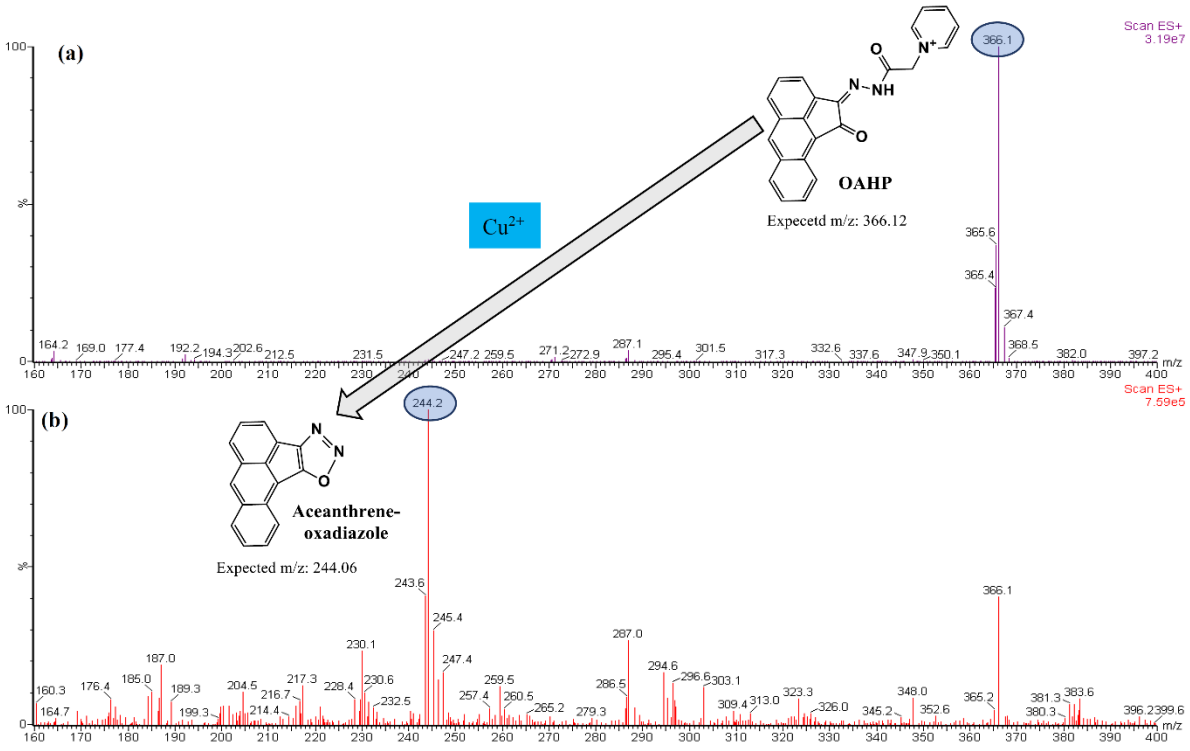

Figure 3. ESI mass spectrum of OAHP (a) before and (b) after its reaction with Cu^{2+}.

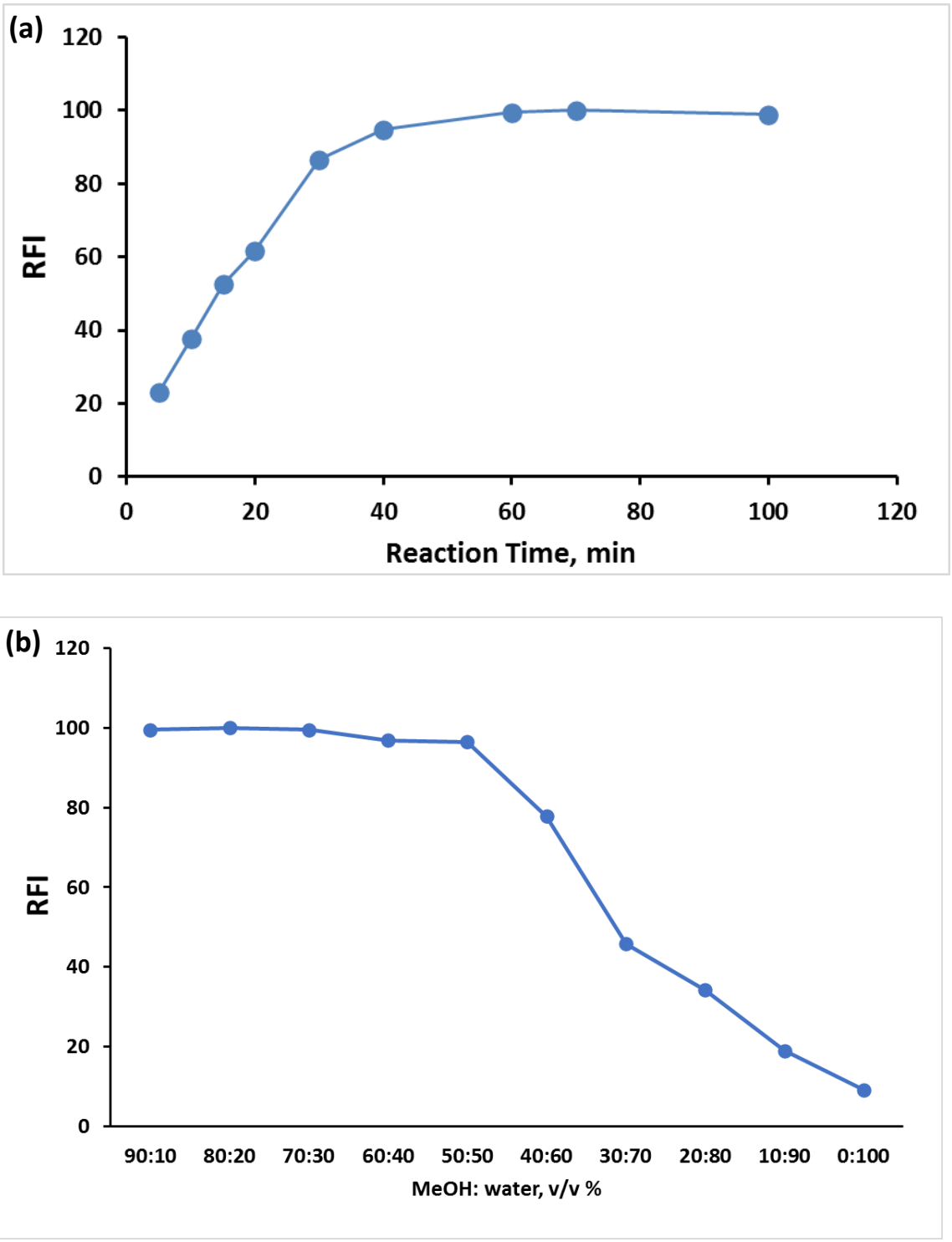

Figure 4. The effect of (a) reaction time and (b) aqueous% of the reaction medium on the obtained fluorescence after reaction of OAHP with Cu^{2+}.

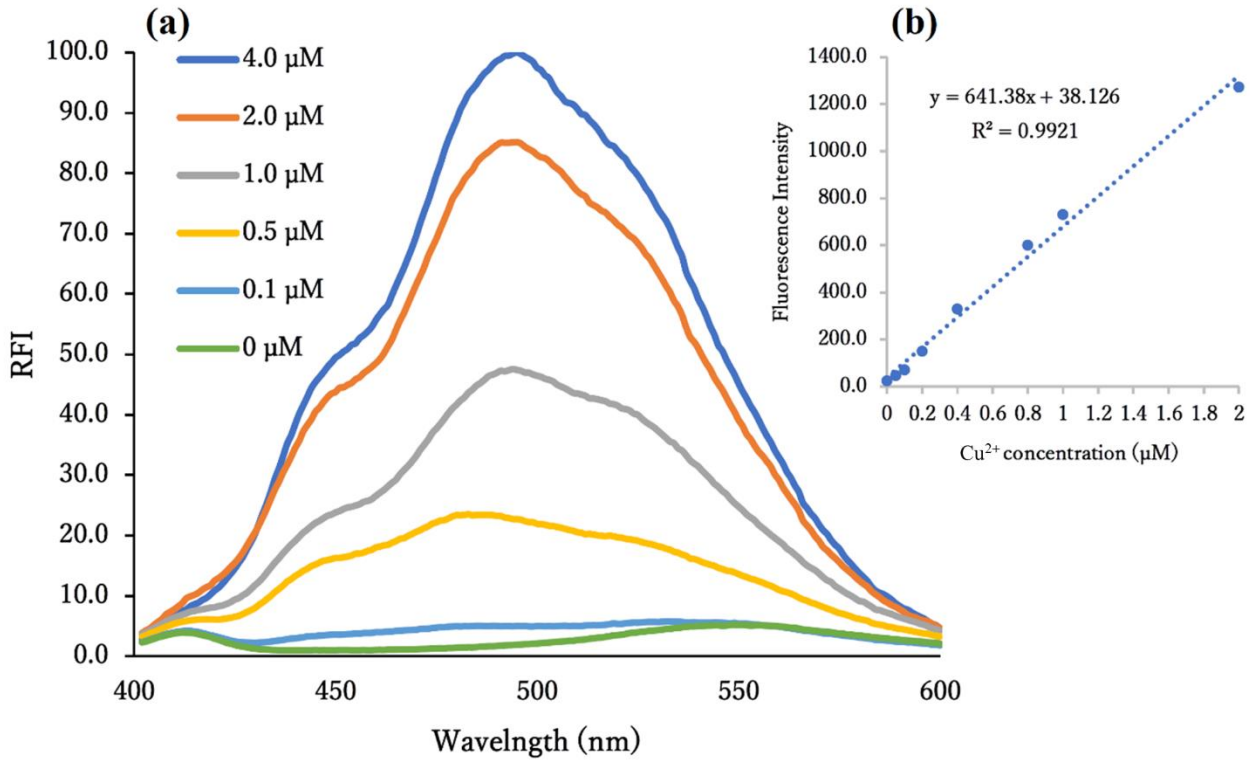

Figure 5. The fluorescence spectra of OAHP (5 µM) in methanol upon addition of different concentration of Cu^{2+} (0, 0.1, 0.5, 1, 2, and 4 µM); λex = 390 nm. (b) Calibration curve and calibration equation for Cu^{2+}.

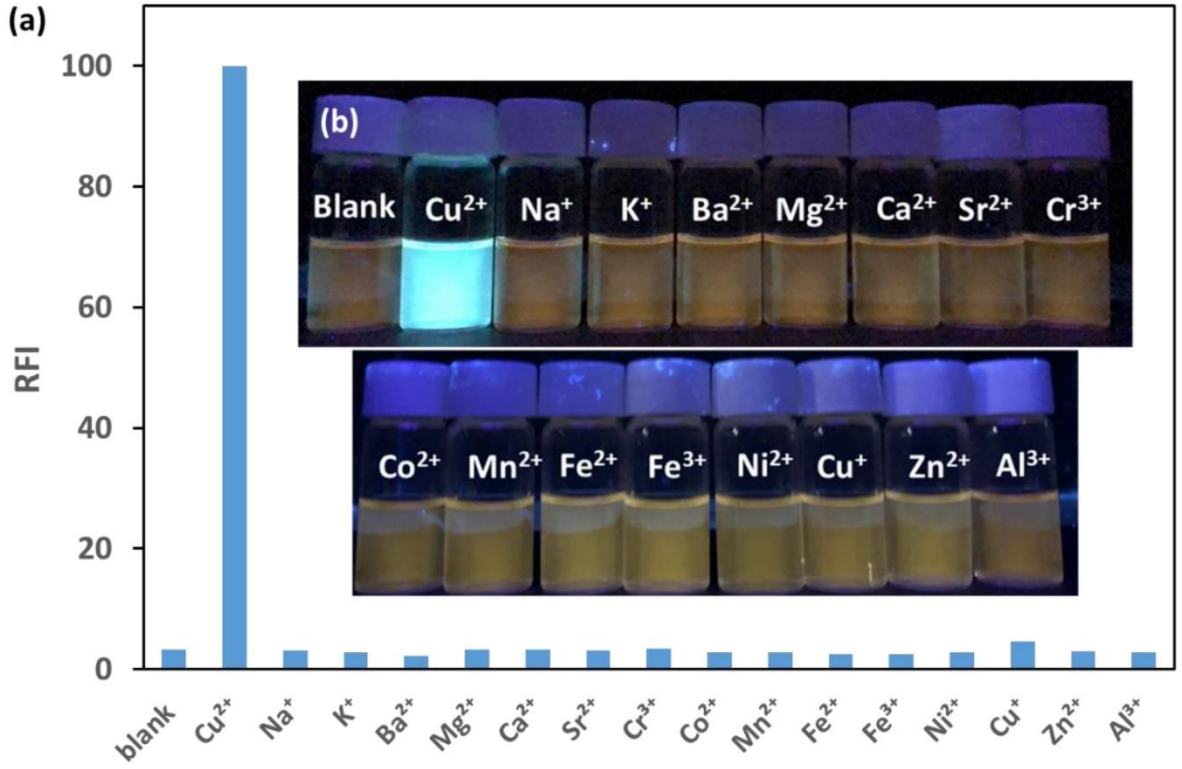

Figure 6. (a) Fluorescence responses of OAHP (50 μM) at 490 nm after adding various metal ions (50 μM for Cu^{2+}, Na^{+}, K^{+}, Ba^{2+}, Mg^{2+}, Ca^{2+}, Sr^{2+}, Cr^{3+}, Co^{2+}, Mn^{2+}, Fe^{2+}, Fe^{3+}, Ni^{2+}, Cu^{+}, Zn^{2+}, and Al^{3+}) at room temperature in methanol. Ex: 370 nm, Em: 490 nm. (b) Photograph of OAHP (50 μM) upon addition of various metal ions (50 μM) with the excitation at 365 nm.

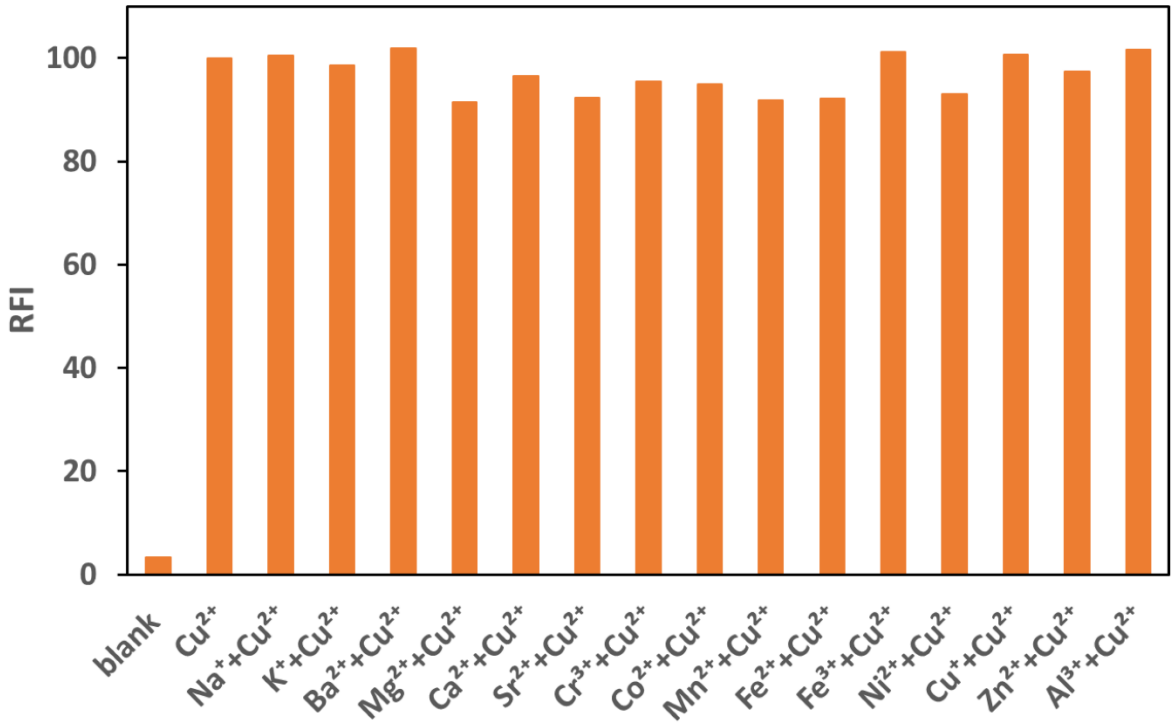

Figure 7. Fluorescence response of OAHP (50 µM) after adding Cu^{2+} (50 µM) and other competing metal ions (50 µM for Cu^{2+}, Na^{+}, K^{+}, Ba^{2+}, Mg^{2+}, Ca^{2+}, Sr^{2+}, Cr^{3+}, Co^{2+}, Mn^{2+}, Fe^{2+}, Fe^{3+}, Ni^{2+}, Cu^{+}, Zn^{2+}, and Al^{3+}) at room temperature in methanol. Ex: 370 nm, Em: 490 nm.

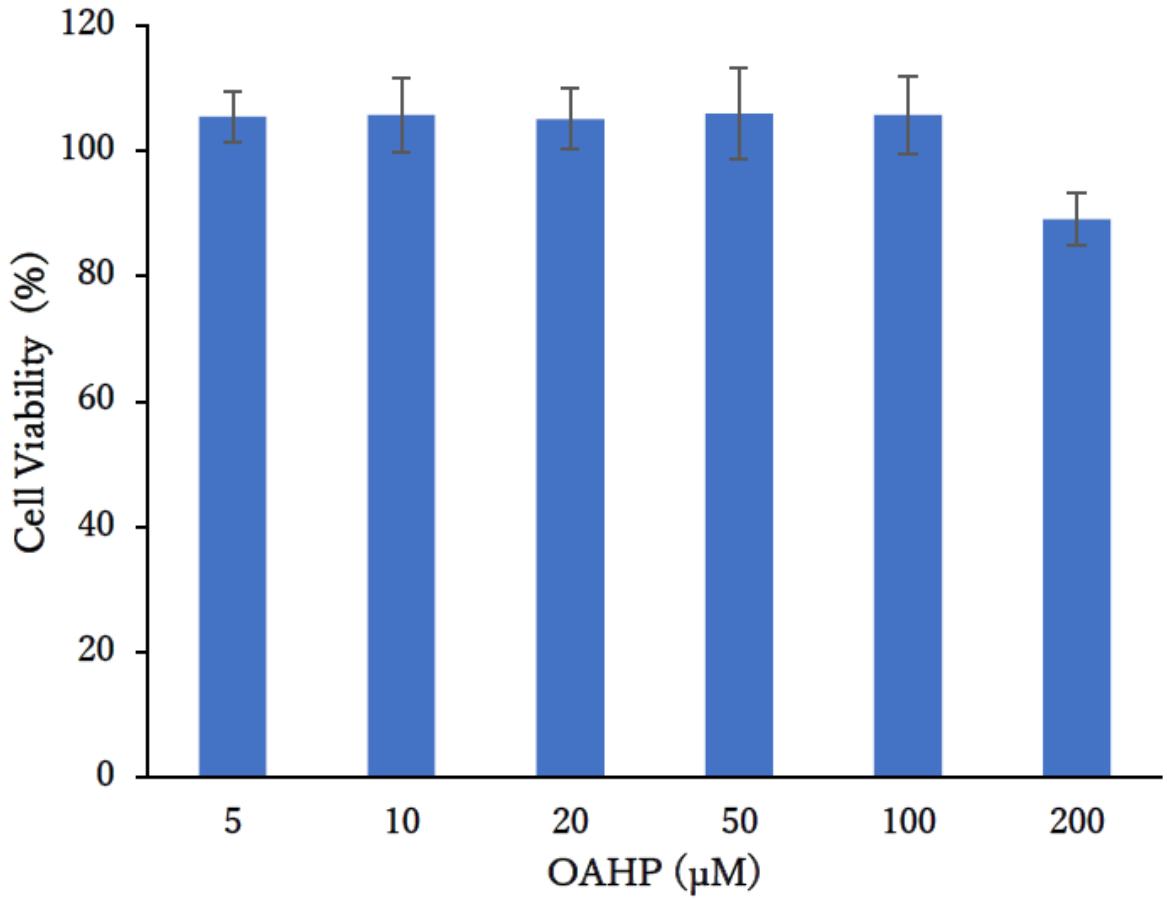

Figure 8. WST-8 assay with different concentrations of OAHP. HepG2 cells were incubated with various concentrations (5, 10, 20, 50, 100, and 200 μM) for 2 hours.

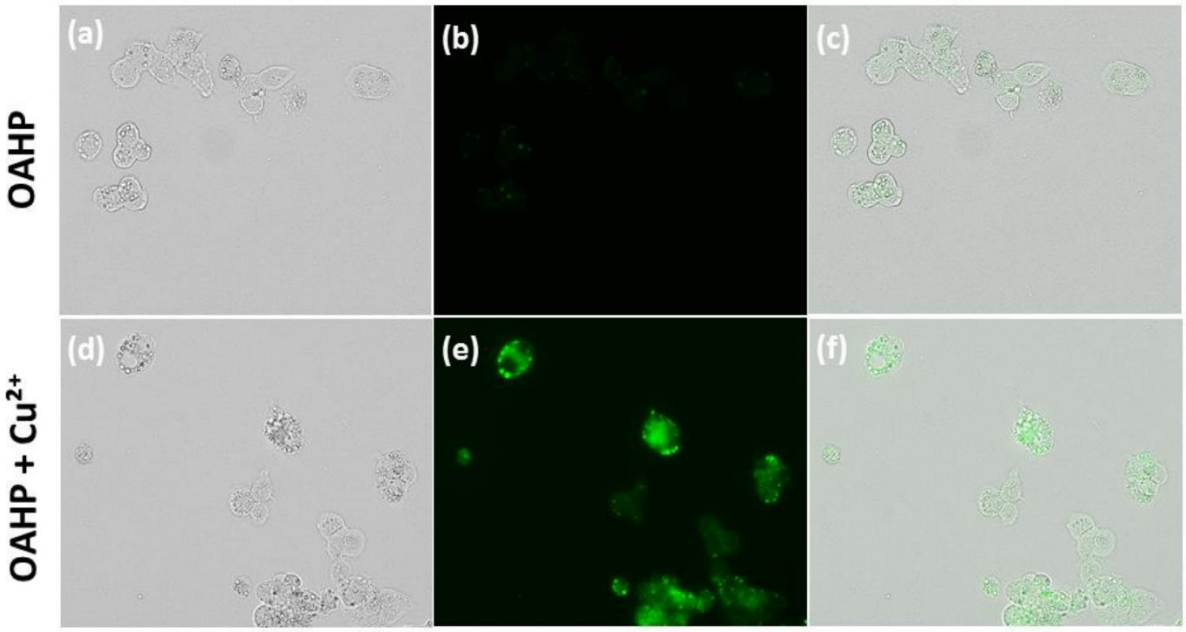

Figure 9. Fluorescence images of Cu^{2+} in HepG2 cells (Ex: 440-470 nm, Em: 525-550 nm). (a) Bright-field images of HepG2 cells after being treated with OAHP (100 μM) for 2 hours. (b) Fluorescence images of a. (c) Overlap of a and b. (d) Bright-field images of HepG2 cells after being treated with Cu^{2+} (100 μM) for 30 min and then incubated with OAHP (100 μM) for 2 hours. (e) Fluorescence images of d. (f) Overlap of d and e.

Supplementary Material

A turn-on hydrazide oxidative decomposition-based fluorescence probe for highly selective detection of Cu^{2+} in tap water as well as cell imaging

Yusuke Okamoto[1], Naoya Kishikawa[2,*], Masayori Hagimori[3], Mahmoud El-Maghrabey[2,4], Shigeru Kawakami[5], Naotaka Kuroda[2]

[1] *School of Pharmaceutical Sciences, Nagasaki University, 1-14 Bunkyo-machi, Nagasaki 852-8521, Japan*

[2] *Department of Analytical Chemistry for Pharmaceutics, Graduate School of Biomedical Sciences, Nagasaki University, 1-14 Bunkyo-machi, Nagasaki, 852-8521, Japan*

[3] *Laboratory of Analytical Chemistry, School of Pharmacy and Pharmaceutical Sciences, Mukogawa Women's University, 11-68 Koshien Kyuban-cho, Nishinomiya 663-8179, Japan*

[4] *Department of Pharmaceutical Analytical Chemistry, Faculty of Pharmacy, Mansoura University, 35116 Mansoura, Egypt*

[5] *Department of Pharmaceutics, Graduate School of Biomedical Sciences, Nagasaki University, 1-7-1 Sakamoto, Nagasaki, 852-8588, Japan*

*** Corresponding author:**

Naoya Kishikawa − *Department of Analytical Chemistry for Pharmaceutics, Graduate School of Biomedical Sciences, Nagasaki University, 1-14 Bunkyo-machi, Nagasaki, 852-8521, Japan;* https://oricd.org/0000-0001-5057-828X; Tel.: +81958192445; fax: +81958192446**;** E-mail address: kishika@nagasaki-u.ac.jp

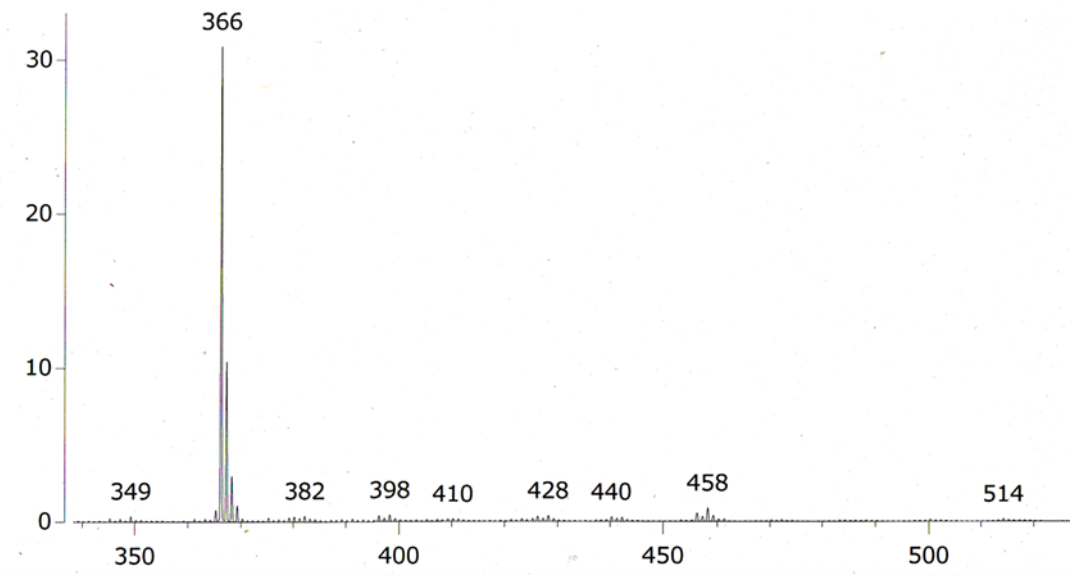

Figure S1: FAB mass spectrum of OAHP.

(a)

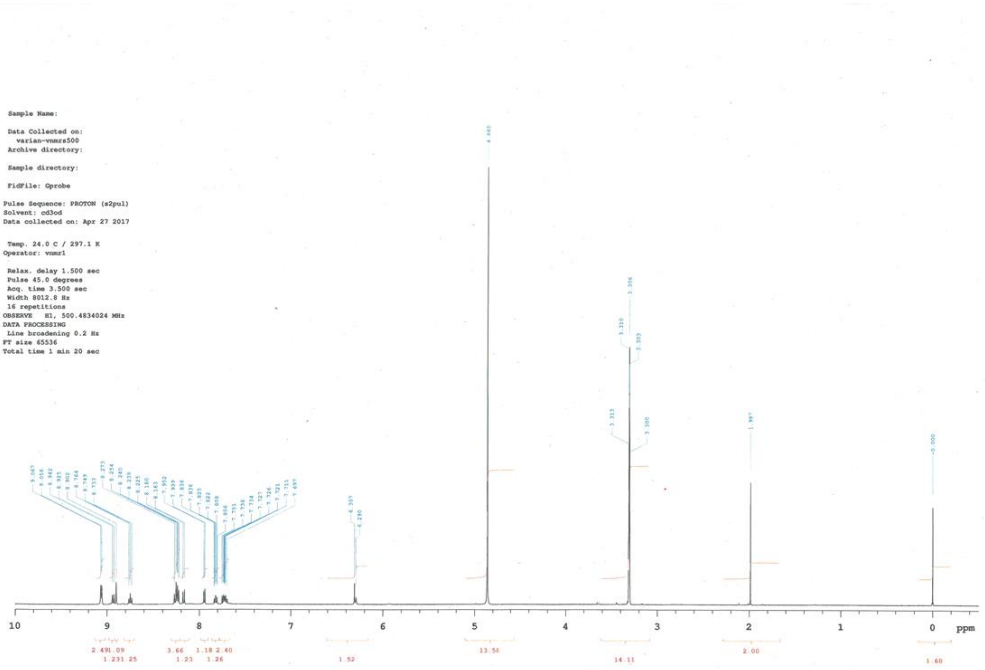

(b)

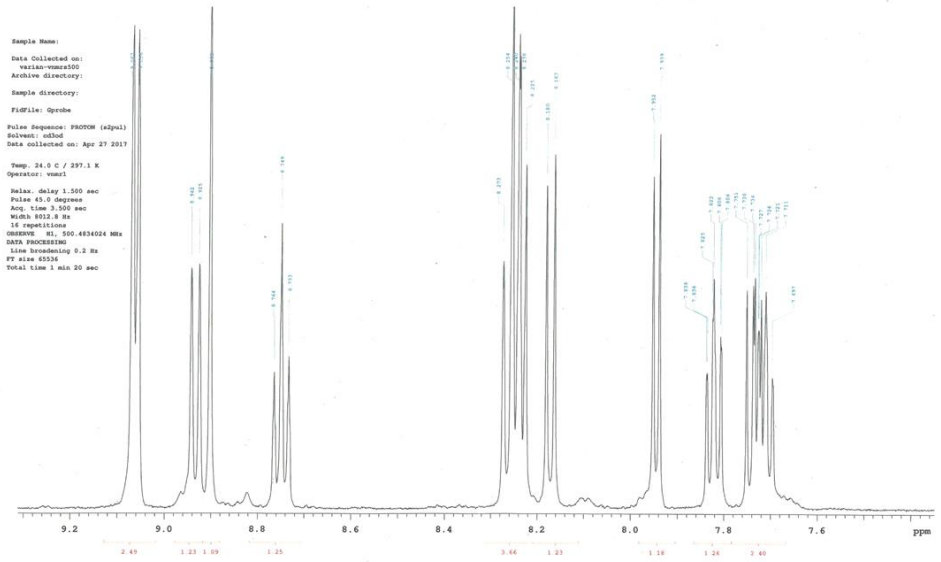

Figure S2: (a) ^{1}H NMR of OAHP. (b) Enlargement of a (7.6-9.2 ppm).

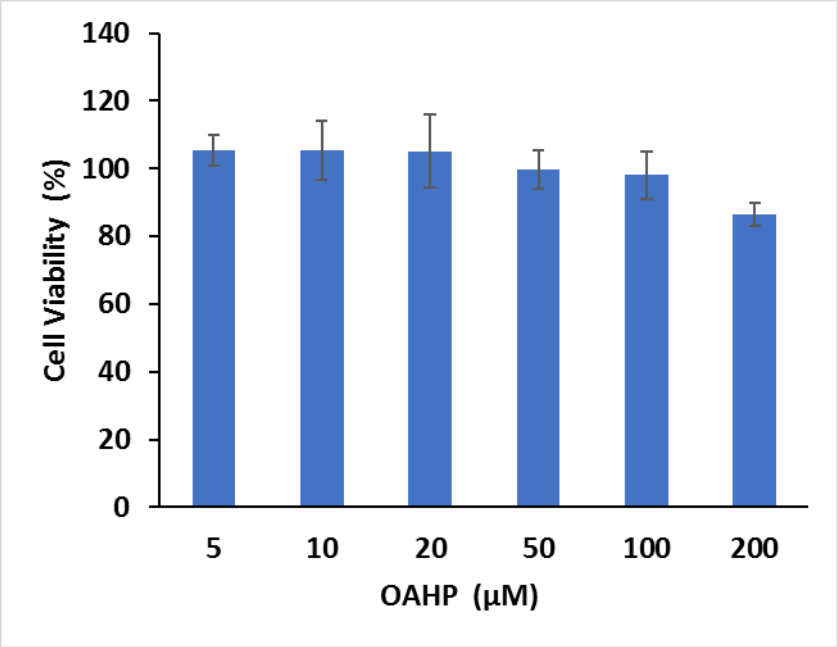

Figure S3. WST-8 assay with different concentrations of OAHP. HepG2 cells were incubated with various concentrations (5, 10, 20, 50, 100, and 200 μM) for 4 hours.

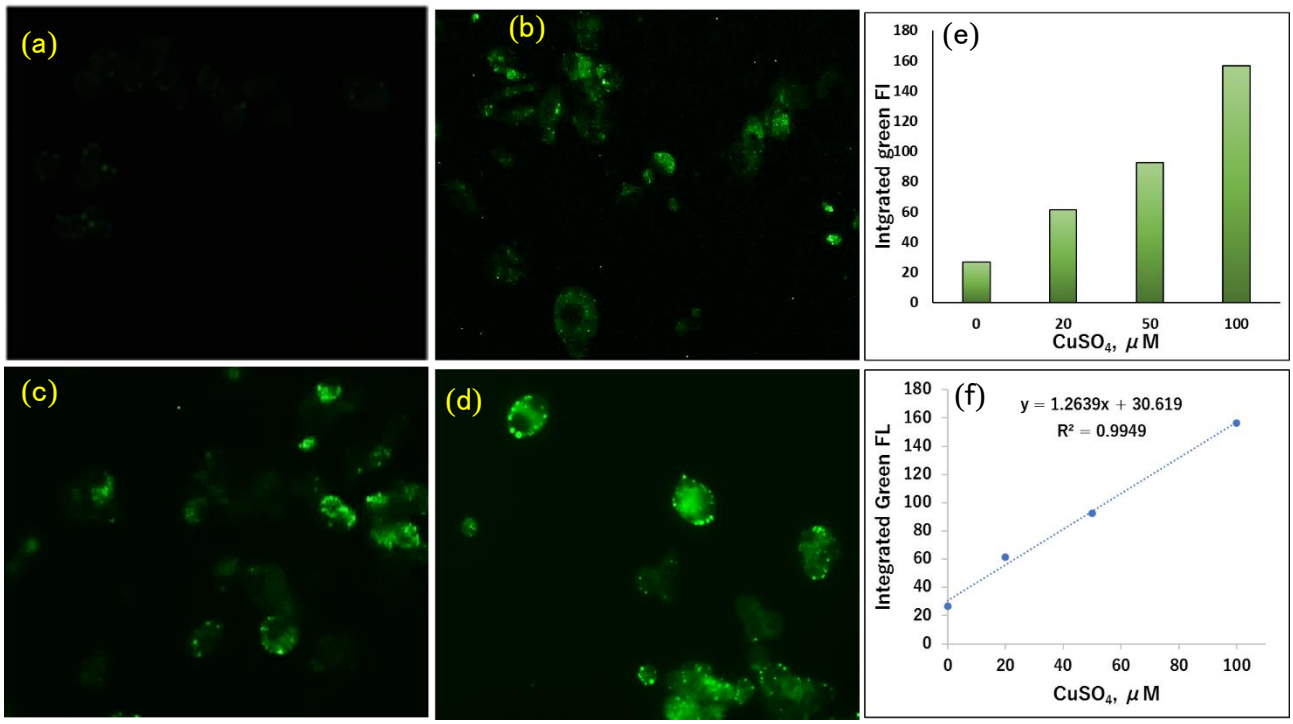

Figure S4: Fluorescence imaging of different concentrations of Cu^{2+} (0 - 100 μM) in HepG2 cells. Where (a), (b), (c), (d) show fluorescence images of Cu^{2+} (0, 20, 50, 100 μM, repeectively) in HepG2 cells (Ex: 440-470 nm, Em: 525-550 nm), (e) and (f) show the integrated green fluorescence intensity of the fluorescence imaging of control and Cu^{2+} treated cells and their calibration curve, respectively.